JPET Fast Forward. Published on November 18, 2009 as DOI: 10.1124/jpet.109.162610

JPET #162610

Role of CYP2A5 in the Clearance of Nicotine and Cotinine: Insights from Studies on a *Cyp2a5*-null Mouse Model

Xin Zhou, Xiaoliang Zhuo, Fang Xie, Kerri Kluetzman, Yue-Zhong Shu, W. Griffith Humphreys, and Xinxin Ding*

Wadsworth Center, New York State Department of Health, and School of Public Health, State University of New York at Albany, Albany, NY (X. Zhou, F.X., K.K., X.D.), Department of Biotransformation, Bristol-Myers Squibb, Wallingford, CT (X. Zhuo, Y.-Z.S.), Department of Biotransformation, Bristol-Myers Squibb, Princeton, NJ (W.G.H.)

Running Title: CYP2A5 and clearance of nicotine and cotinine

Send correspondence and galley proofs to:

Dr. Xinxin Ding
Wadsworth Center, New York State Department of Health
Empire State Plaza, Box 509
Albany, NY 12201-0509
Phone: 518-486-2585
Fax: 518-473-8722
Email: xding@wadsworth.org

Number of Text Pages: 26

Number of Tables: 5

Number of Figures: 3

Number of References: 40

Number of words: Abstract 250

Introduction 739

Discussion 1472

Abbreviations: P450, cytochrome P450; CPR, cytochrome P450 reductase; UGT, UDP-glucuronosyltransferase; PCR, polymerase chain reaction; RT, reverse transcription; HPLC, high performance liquid chromatography; kb, kilobase pair; MS, mass spectrometer; AUC, area under the concentration; C_{max}, maximal concentration; T_{max}, time at maximal concentration; $t_{1/2}$, elimination half-life; CL, clearance; F, bioavailability; NADPH, reduced β-nicotinamide adenine dinucleotide phosphate; cotinine-d_3, (±)-cotinine-methyl-d_3.

Section assignment: Metabolism, Transport, and Pharmacogenomics

Abstract

CYP2A5, a mouse cytochrome P450 monooxygenase that shows high similarities to human CYP2A6 and CYP2A13 in protein sequence and substrate specificity, is expressed in multiple tissues, including the liver, kidney, lung, and nasal mucosa. Heterologously expressed CYP2A5 is active in the metabolism of both endogenous substrates, such as testosterone, and xenobiotic compounds, such as nicotine and cotinine. To determine the biological and pharmacological functions of CYP2A5 in vivo, we have generated a *Cyp2a5*-null mouse. Homozygous *Cyp2a5*-null mice are viable and fertile; they show no evidence of embryonic lethality or developmental deficits; and they have normal circulating levels of testosterone and progesterone. The *Cyp2a5*-null mouse and wild-type mouse were then utilized for determination of the roles of CYP2A5 in the metabolism of nicotine and its major circulating metabolite, cotinine. The results indicated that the *Cyp2a5*-null mouse has lower hepatic nicotine 5'-hydroxylation activity in vitro, as well as slower systemic clearance of both nicotine and cotinine in vivo. For both compounds, a substantially longer plasma half-life, and a greater area under the concentration-time curve, were observed for the *Cyp2a5*-null mice, as compared with wild-type mice. Further pharmacokinetics analysis confirmed that the brain levels of nicotine and cotinine are also influenced by the *Cyp2a5* deletion. These findings provide direct evidence that CYP2A5 is the major nicotine and cotinine oxidase in mouse liver. The *Cyp2a5*-null mouse will be valuable for in vivo studies on the role of CYP2A5 in drug metabolism and chemical toxicity, and for future production of CYP2A6 and CYP2A13-humanized mouse models.

Introduction

The mouse *Cyp2a* gene subfamily encompasses four genes (*Cyp2a4*, *Cyp2a5*, *Cyp2a12*, and *Cyp2a22*), whereas the human *CYP2A* gene subfamily has three genes (*CYP2A6*, *CYP2A7*, and *CYP2A13*) (Wang et al., 2003). Human CYP2A6 and CYP2A13 are known to be functional, and they are most similar to mouse CYP2A5, with respect to tissue distribution and substrate specificity (Su et al., 2004). Both CYP2A6 and CYP2A13 are expressed in the olfactory mucosa (OM) and other tissues of the respiratory tract, while CYP2A6 is also expressed in the liver; mouse CYP2A5 is expressed in many tissues, including tissues of the respiratory tract, liver, and kidney. CYP2A5 shares many substrates with CYP2A6 and/or CYP2A13, such as coumarin, nicotine, cotinine, testosterone, as well as the tobacco-specific carcinogen 4-(methylnitrosamino)-1-(3-pyridyl)-1-butanone and other nitrosamines (Su et al., 2004; Wong et al., 2005; Raunio et al., 2008a).

Nicotine is the pharmacologically active (and addictive) ingredient in cigarette products. Nicotine is also used as a therapeutic agent for smoking cessation, and it is being tested as a potential preventative agent for neurodegenerative diseases, both in animal models and in clinical trials (Quik et al., 2007; Ravina et al., 2003). Nicotine can be metabolized via several pathways in humans, including 5'-hydroxylation to yield cotinine, catalyzed mainly by CYP2A6 (Nakajima et al., 1996; Messina et al., 1997); N-demethylation (Murphy et al., 2005), also mediated by CYP2A6; N-oxidation (Cashman et al., 1992**;** Cashman 2000), catalyzed by flavin-containing monooxygenase; and N-glucuronidation (Kuehl et al., 2003; Kaivosaari et al., 2007), catalyzed by various UDP-glucuronosyltransferases. In humans, ~75% of administered nicotine is converted to cotinine (Hukkanen et al., 2005), a gamma lactam metabolite formed via 5'-hydroxylation. Indeed, cotinine is used as a chemical marker for human exposure to cigarette smoking (de Leon et al., 2002). Additionally, genetic polymorphisms in the human *CYP2A6*

gene have been linked to inter-individual differences in the rates of nicotine clearance (Benowitz et al., 2006).

Mouse CYP2A5 is also believed to play a major role in the clearance of nicotine and cotinine, based on in vitro data and in vivo pharmacological evidence (Raunio et al., 2008b; Siu et al., 2006; Siu and Tyndale, 2007), although direct in vivo evidence, such as the disposition in a *Cyp2a5*-null mouse, has yet to be reported. However, a remarkable species difference exists between humans and mice in the rates of nicotine clearance, with the metabolism being much more rapid in mice than in humans. This notable species difference makes it difficult to extrapolate pharmacological and toxicological findings obtained in mouse experiments to human contexts. Furthermore, the rapid metabolism of nicotine in mice has hindered efforts to use this species for studies on the mechanisms of nicotine addiction, or for studies on the potential of nicotine as an agent for prevention of diseases such as Parkinson's disease (Quik et al., 2007). Biochemical studies have suggested that the species difference between mouse and humans in nicotine clearance is largely due to differences in the efficiencies of human CYP2A6 and mouse CYP2A5 in nicotine 5'-hydroxylation, with CYP2A5 being much more efficient than is CYP2A6 (Murphy et al., 2005). Indeed, other mouse hepatic P450 enzymes appear to be either similar to, or less efficient than, human CYP2A6, with respect to their enzymatic activities toward nicotine (Murphy et al., 2005; Siu and Tyndale et al., 2007). Thus, a *Cyp2a5*-null mouse will not only be valuable for determination of the specific roles of CYP2A5 in drug metabolism and toxicity in a mouse model, but it will also represent a more "humanized" mouse model that is suitable for various studies concerning the pharmacology of nicotine and cotinine. A *Cyp2a5*-knockout mouse model has not been described previously.

In the present study, we have generated a *Cyp2a5*-null mouse through homologous recombination in embryonic stem (ES) cells derived from the C57BL/6 (B6) mouse strain.

Homozygous *Cyp2a5*-null mice were characterized for: viability and fertility; growth rates; potential compensatory expression in other enzymes that can influence nicotine clearance; and circulating levels of testosterone and progesterone, endogenous compounds that are among known CYP2A5 substrates. The *Cyp2a5*-null mice were then compared to the WT B6 mice, for their abilities to clear nicotine and cotinine in vivo, and for the activities of their hepatic microsomes to metabolize nicotine in vitro. Pharmacokinetic analyses were then performed, to determine the impact of the *Cyp2a5* deletion on levels of nicotine and cotinine in the brain (the pharmacological target organ), the liver (the major site of metabolic clearance), and the blood (the medium for biomonitoring).

Methods

Chemicals and reagents. (-)-cotinine, (±)-cotinine-methyl-d_3 (cotinine-d_3), (-)-nicotine hydrogen tartrate, (-)-nicotine, ammonium acetate, and NADPH were purchased from Sigma-Aldrich (St. Louis, MO). The sources of testosterone, progesterone, 16α-hydroxy-progesterone, and all testosterone metabolite standards were the same as described previously (Ding and Coon 1988; 1994; Zhou et al., 2009). 3,4-^{13}C-progesterone was obtained from Cambridge Isotope Laboratories (Andover, MA). All solvents (acetonitrile, methanol, and water) were of high-performance liquid chromatography (HPLC) grade (Fisher Scientific, Houston, TX).

Targeting vector construction. The targeting vector (Fig. 1) was prepared in a pMC-lox-neo-lox vector (4.0 kb) (Millipore, Billerica, MA). It consists of a *tk-neo*-bpA cassette for the neomycin-resistance (*neo*) gene expression, using the thymidine kinase (*tk*) promoter; the *neo* was flanked by two loxP sites in the same orientation. A 1.6-kb Pst I fragment encompassing exons 6-8, and a 5.6-kb BamH I-EcoR I fragment of the 3'-flanking region, were obtained from the C57BL/6 (B6) mouse bacterial artificial chromosome (BAC) clone RP23-165I8 (BACPAC Resources, Oakland, CA), which contains *Cyp2a5*, but not *Cyp2a4*. The two fragments were cloned into the pMC-lox-neo-lox vector, which was linearized with Cla I, before electroporation into embryonic stem (ES) cells.

Electroporation and selection of ES cells. The Bruce4 (C57BL/6J-derived) ES cells (Kontgen et al., 1993), kindly provided by Dr. Colin Stewart (National Cancer Institute, Frederick, MD), were used for electroporation, at the Transgenic and Knockout Core Facility of the Wadsworth Center. Recombinant ES cells were selected with the use of 250 μg/ml G418. Positive ES cell clones were identified by PCR [using the primers 5'-ttagggcactgggtcacttc-3' (upstream of the 1.6-kb Pst I fragment) and 5'-cgatctagaggtaccataacttcgt-3' (within the vector region), with an annealing temperature of 62°C], and was confirmed by Southern blot analysis

with both internal (a 350-bp Hind III-Pst I fragment upstream of the Pvu II restriction site within the targeting vector) and external probes (an 1.1-kb BamH I-Sac I fragment upstream of exon 6 of the *Cyp2a5* gene).

Blastocyst injection and animal breeding. ES cells from positive clones were karyotyped, and the clone with the best karyotyping result was selected for expansion. ES cells were injected into the blastocysts from albino B6(Cg)-Tyrc-2J/J (Jackson Laboratory) female mice. Blastocysts were transferred into the uterus of a pseudopregnant B6CBAF1/J mouse, for generation of offspring. Male chimera pups were identified by their black eyes and coat color. Adult chimeras were bred with C57BL/6J female mice, in order to produce germline-transmission F1 mice that were heterozygous for the *Cyp2a5*-null allele. F2 homozygotes were used for breeding and characterization. B6 mice were used as WT controls in all experiments described. All procedures involving animals were approved by the Institutional Animal Care and Use Committee of the Wadsworth Center.

RNA-PCR. Tissues for RNA or microsome preparation were all collected between 9:00 and 10:00 A.M. local time. Total RNA was isolated with use of the RNeasy Mini kit (QIAGEN, Valencia, CA). All RNA samples were treated with DNase I (Life Technologies, Carlsbad, CA) before reverse transcription (RT). RNA-PCR analysis was performed as previously described (Zhang et al., 2005). Gene-specific PCR primers for amplification of exons 2 and 3 of *Cyp2a5* were the same as described elsewhere (Zhuo et al., 2004); the primers for amplification of exons 8 and 9 were 5’-gatgacaagggacagtttaagaagaa-3’and 5’-gtgtaggttggtgggatcgtgg-3’ (with an annealing temperature of 66°C). PCR products were validated by sequence analysis. Methods for real-time PCR analysis of CYP2G1 and CYP2A12 expression are described in the Supplemental Materials.

Pharmacokinetic analysis for nicotine and cotinine. For studies on systemic clearance of nicotine and cotinine, mice were given a single i.p. injection (at 9-10 a.m.) of either nicotine tartrate (at 1.0 or 5.0 mg/kg, free base) or cotinine (at 1.0 mg /kg) in saline. Blood samples (~20 µl each) were collected from the tail of individual mouse, at various time points (5 min to 8 h) after the injection. The samples were centrifuged at 1000 *g*, for 5 min, at 4°C, for preparation of plasma. For studies on tissue nicotine and cotinine levels, tissue samples, as well as blood samples (from the heart), were obtained after animals were killed by CO_2 asphyxiation. Pharmacokinetics parameters were calculated using the noncompartmental method in the WinNonlin software (Pharsight, Mountain View, CA). Statistical significance of differences between two groups was examined with Student's *t*-test. For total body clearance, the hybrid constant CL/F was used, according to Statler and coworkers (Statler et al., 2007), instead of CL (clearance), given that F (bioavailability) is not known.

For plasma samples, 0.1 ng cotinine-d_3 was added as internal standard to 10 µl of plasma, which had been diluted in 1.0 ml 0.6 M phosphate buffer, pH 6.8, as described before (Heavner et al., 2005). The resultant mixture was extracted with an Isolute Extraction Cartridge (C18; 1 ml/100 mg) (Biotage, Charlottesville, VA). The samples were eluted with 1 ml methanol, dried under nitrogen, and then reconstituted with 50% (v/v) methanol in water for LC/MS analysis. The recovery of added nicotine and cotinine standards in blank plasma was > 80%, at all concentrations tested. For tissue sample preparation, brain and liver (~ 400 mg each) were homogenized in 3 ml saline (0.9% NaCl), followed by addition of 0.1 ng cotinine-d_3. The mixtures were centrifuged, at 3000 g, for 10 min, and the supernatant was then extracted with an Isolute Extraction Cartridge (C18; 3 ml/100 mg), as described above for plasma samples. The recovery of added standards in blank tissues was >75%, at all concentrations tested.

The levels of nicotine and cotinine were determined using a LC/MS system composed of an Agilent 1200 Series HPLC and an ABI 4000 Q-Trap mass spectrometer (Applied Biosystems, Foster City, CA), fitted with a 5-µm Gemini C18 column (50 x 2.0 mm). The samples were eluted at a flow rate of 0.2 ml/min, with solvent A (10 mM ammonium acetate in water) and solvent B (100% acetonitrile); the column was equilibrated with 100%A for 1 min, and the solvent gradient consisted of linear increases from 0%B to 100%B between 1 and 8 min, followed by a wash at 100%B for 1 min. The MS was operated in the positive ion mode, using electrospray ionization (ESI). The parent/product ion pairs of *m/z* 163/130 (for nicotine), *m/z* 177/80 (for cotinine), and *m/z* 180/80 (for cotinine-d_3) were monitored in the Multiple Reaction Monitoring scan mode. The parameters for the chamber were as follows: curtain gas, 40 psig; heated nebulizer temperature, 350°C; ion spray voltage, 4000 V; nebulizer gas, 50 psig; turbo gas, 50 psig, declustering potential, 40 V; and entrance potential, 10 V. For both compounds, the detection limit was 0.5 pg/µl, or 5 pg on column.

Identification of hepatic microsomal nicotine metabolites by LC/MS. Assay mixtures contained 50 mM potassium phosphate buffer, pH 7.4, 10 µM nicotine, 1.0 mg/ml liver microsomal protein, with or without 1 mM potassium cyanate (KCN), and 1.0 mM NADPH, in a final volume of 0.3 ml. Reactions were carried out at 37°C for 0 or 60 min, and were terminated by the addition of 0.3 ml acetonitrile, followed by removal of denatured proteins through centrifugation. The supernatant was analyzed using an LC/UV/MS system consisting of a Waters 2690 separation module (Waters, Milford, MA), a Surveyor photodiode array (PDA) detector (ThermoFisher Scientific, Waltham, MA), and an LCQ Deca XP ion-trap mass spectrometer (ThermoFisher Scientific). The chromatographic separation of metabolites was achieved on a 5-µm Gemini C18 (150 x 2.0 mm) column (Phenomenex, Torrance, CA). The mobile phase consisted of solvent A (10 mM ammonium acetate in water) and solvent B (100% acetonitrile).

The samples were eluted, at a flow rate of 0.5 ml/min, with 100% A for 20 min, followed by linear increases from 0% B to 100% B between 21 and 25 min, and then 100% B for a further 10 min. The mass spectrometer was set for a data-dependent scan mode, and was operated in a positive ion mode with an atmospheric pressure chemical ionization (APCI) source. The parameters for the chamber were: *m*/*z* range, 50 to 500; capillary temperature, 350°C; nitrogen sheath gas flow rate, 30 (arbitrary units); auxiliary gas, 10 (arbitrary units); spray voltage, 4 kV; capillary voltage, 10 V; and tube lens offset, 30 V.

In vitro metabolism of testosterone and nicotine. Microsomal preparation was carried out essentially as described previously (Ding and Coon, 1990); the post-microsomal supernatant fraction was used as cytosol. Metabolism of testosterone was assayed essentially as described previously (Zhou et al., 2009). Reaction mixtures contained 5.0 or 10 μM testosterone and 0.1 mg/ml liver microsomal protein, and the reaction was carried out for 10 min. Testosterone metabolites were identified using a LC/MS system consisting of an Agilent 1200 Series HPLC and an ABI 4000 Q-Trap mass spectrometer, essentially as described elsewhere (Zhou et al., 2009), with minor modifications, as detailed in the Supplemental Materials. For assay of nicotine C-5'-oxidation, the reaction mixture contained 1.0 or 10 μM nicotine, 0.5 mg/ml liver microsomal protein, and 1.0 mg/ml cytosolic protein. The reactions were carried out under conditions that support constant rates of product formation, according to a protocol described previously (Siu et al., 2006). The reaction was stopped by the addition of 1 ml methanol (containing 1 ng cotinine-d_3), and the mixture was centrifuged, in order to precipitate protein. The supernatant was dried under nitrogen, and then reconstituted with 50% (v/v) methanol in water, for the measurement of cotinine by LC/MS analysis (as described above for the pharmacokinetics of plasma cotinine). Metabolite standard was added to reaction mixtures containing boiled microsomes, with recoveries being > 85% at all concentrations tested.

JPET Fast Forward. Published on November 18, 2009 as DOI: 10.1124/jpet.109.162610
This article has not been copyedited and formatted. The final version may differ from this version.

Quantitative analysis of serum testosterone and progesterone by LC/MS. Two-month-old male and female mice were respectively used for testosterone and progesterone determination. For serum testosterone**,** samples were prepared and analyzed essentially as described previously (Zhou et al., 2009). For serum progesterone, the sample preparation method was modified from the protocol of Tai and coworkers (Tai et al., 2006). The internal standard, 3,4-^{13}C-progesterone, was added to serum samples at 1.0 ng/ml. Samples were extracted twice, each time with 10 volumes of hexane; the extracts were dried with nitrogen, and then reconstituted in 50% methanol for LC/MS analysis. To construct calibration curves, we added progesterone and stable isotope-labeled progesterone to charcoal-stripped bovine serum (Hyclone, Logan, UT). The recovery of added progesterone was > 90%, at all concentrations tested. Details of LC/MS analysis for progesterone are included in the Supplemental Materials.

Results

Generation and characterization of the *Cyp2a5*-null mouse

The structures of the WT *Cyp2a5* allele, the targeting construct, and the targeted *Cyp2a5*-null allele are shown in Figure 1 (panels A, B, and C). A *Cyp2a5* BAC genomic clone, isolated from the B6 strain, was used for construction of the targeting vector. The strategy used for targeted disruption of the mouse *Cyp2a5* gene by homologous recombination in ES cells was to replace the last exon (exon 9), which encodes the active-site CYS residue, with a neomycin-resistance gene. ES cells from a homologous recombinant clone (clone #221) were used for subsequent injection into the blastocyst cavity of albino B6(Cg)-Tyrc-2J/J embryos, from which a chimeric male was generated. When bred with WT B6 females, the chimera exhibited germline transmission. The absence of random integration of the targeting construct was confirmed by the use of both internal (Probe I) and external (Probe E) probes for Southern blot analysis (data not shown). Homozygous *Cyp2a5*-null mice (*Cyp2a5*$^{-/-}$) were produced by crossbreeding between heterozygous littermates (*Cyp2a5*$^{+/-}$). Homozygotes, heterozygotes, and WT littermates were identified by the presence of the characteristic bands for the WT (7-kb) and the *Cyp2a5*-null (4-kb) alleles, on Southern blots (Fig. 1D). As a control, the integrity of the *Cyp2a4/12* genes, which are highly similar to *Cyp2a5* in genomic structure, is confirmed by the detection of the unique 2-kb genomic fragment, in mice of all three genotypes.

The absence of *Cyp2a5* expression in various tissues of the *Cyp2a5*-null mice was confirmed by RNA-PCR, with use of two sets of gene-specific primers, which are complementary to sequences near either the 5'-end (E2-E3) or the 3'-end (E8-E9) of the CYP2A5 transcript. The results (Fig. 1E) indicated that neither the full-length CYP2A5 mRNA, nor a truncated CYP2A5 mRNA containing the first eight exons (which are intact), was present at detectable levels, in any of the tissues examined, of either male or female *Cyp2a5*-null mice.

Mice homozygous for the disrupted allele were indistinguishable from their WT littermates, or from WT B6 mice, in growth rate and reproductive ability. No deviation from Mendelian distribution of genotypes was observed in pups derived from F1 heterozygous breeding pairs (Supplemental Table 1), a result suggesting that CYP2A5 is not critical for embryonic development. Adult body and organ weights (liver, kidney, lung, and testis for males, and liver, kidney, and lung for females) were identical between *Cyp2a5*-null and WT B6 mice (Supplemental Table 2), indicating that CYP2A5 is not essential for normal growth. Homozygous breeding pairs were established, to produce *Cyp2a5*-null mice for subsequent studies.

Given our previous finding of a neighboring effect of *Cyp2g1* gene disruption on the expression of the [downstream] *Cyp2a5* gene (Zhuo et al., 2004), we examined the potential effects of the disruption to *Cyp2a5*, on the expression of the neighboring *Cyp2g1*. We found that there was no significant difference between *Cyp2a5*-null and WT mice, in CYP2G1 mRNA levels in the olfactory mucosa, a site where CYP2G1 is uniquely expressed (Supplemental Fig. 1). Thus, the genomic disruption at *Cyp2a5* exon 9 did not lead to noticeable changes in the expression of the upstream *Cyp2g1* gene.

The expression of various *Cyp2b* genes, which are located further upstream of the *Cyp2g1* gene, also appeared to be unaffected by the *neo* insertion, as exemplified by the results from immunoblot analysis of CYP2B protein expression (Supplemental Figure 2). Notably, immediately downstream of *Cyp2a5* is a cluster of *Cyp2a* genes and pseudogenes, including (in order of increasing distance from *Cyp2a5*) *Cyp2a23-ps*, *Cyp2a22*, *Cyp2a21-ps*, *Cyp2a12*, and *Cyp2a20-ps*, with *Cyp2a23-ps*, a pseudogene, located at a distance of >100 kb from *Cyp2a5* (Wang et al., 2003). The expression of *Cyp2a22*, a gene immediately downstream of *Cyp2a23-ps*, was not detected in the liver of either WT or *Cyp2a5*-null mice (data not shown); there has been

no previous report of studies on *Cyp2a22* expression or function. Thus, the first functional gene downstream of *Cyp2a5* is *Cyp2a12* (Su et al., 2004). Hepatic expression of *Cyp2a12* was also not different between WT and *Cyp2a5*-null mice (data not shown), thus further confirming the absence of any neighboring effects of the *neo* insertion.

To examine whether the loss of *Cyp2a5* expression in the liver led to compensatory increases in the expression of other biotransformation genes, we compared hepatic microsomal levels of several P450 proteins, namely, CYP2B, 2C, and 3A, as well as CPR, UGT1A, and UGT2B proteins, between *Cyp2a5*-null and WT mice. We found that the expression levels were similar between WT and *Cyp2a5*-null mice for each of these enzymes, in liver microsomes (Supplemental Fig. 2). Furthermore, we examined the metabolism of testosterone, a common substrate for multiple P450 enzymes, in liver microsomal reactions (Table 1). We found that, whereas the rates of formation of 15β-OH-testosterone, a testosterone metabolite known to be produced by CYP2A5, were lower (by ~50%), the rates of formation of two major testosterone metabolites, 16α-OH-testosterone and 6β-OH-testosterone, the respectively preferred products formed by CYP2D9 (Wong et al., 1987) and CYP3A (Yanagimotoy et al., 1992), were not changed, in the *Cyp2a5*-null mice, as compared to WT mice. In other studies not shown, we also observed lower rates of formation of 15α-OH-testosterone (also a CYP2A5 product), but not 16β, 6α, or 11α-OH testosterone. Consistent with the lack of a substantial difference in the overall rate of hepatic microsomal testosterone metabolism in vitro, there was no significant difference in circulating testosterone levels between WT males and *Cyp2a5*-null males (Supplemental Fig. 3A). Similarly, there was also no significant difference in circulating progesterone levels between WT females and *Cyp2a5*-null females (Supplemental Fig. 3B). These in vivo results indicate that, although CYP2A5 is active toward testosterone and progesterone (Gu et al., 1999),

JPET Fast Forward. Published on November 18, 2009 as DOI: 10.1124/jpet.109.162610
This article has not been copyedited and formatted. The final version may differ from this version.

it does not play a major role in the systemic clearance of testosterone or progesterone in the WT mice.

Role of CYP2A5 in the metabolic clearance of nicotine and cotinine

Systemic clearance of nicotine was compared between *Cyp2a5*-null and WT mice, with nicotine administered at either 1 mg/kg (Fig. 2A) or 5 mg/kg (Fig. 2B). As expected, clearance of nicotine in the WT mouse was very rapid, with a $t_{1/2}$ value of ~13 min following an i.p. injection at a dose of 1 mg/kg, and a $t_{1/2}$ value of ~70 min following an i.p. injection at the higher dose, 5 mg/kg (Table 2). Nicotine clearance was significantly slower (by >70% in CL/F values) in the *Cyp2a5*-null mice, with concomitant 3.2-fold and 6.1-fold increases in the values for C_{max} and AUC, respectively, at a dose of 1 mg/kg, and 3.4-fold and 2.7-fold increases in the values for C_{max} and AUC, respectively, at a dose of 5 mg/kg. Increases in the $t_{1/2}$ value were also observed: 2.8-fold and 1.4-fold, for nicotine doses of 1 mg/kg and 5 mg/kg, respectively. Consistent with the notion that CYP2A5 is the low-Km enzyme in metabolizing nicotine, the impact of *Cyp2a5* deletion on nicotine clearance was more pronounced at the 1 mg/kg dose than at the 5 mg/kg dose, as indicated by the greater magnitude (low-dose group vs high-dose group) of differences between null and WT mice, in both AUC (6.1-fold vs 2.7-fold, respectively) and $t_{1/2}$ (2.8-fold vs 1.4-fold, respectively). A further examination of the AUC values obtained at the two nicotine doses indicated a greater difference in the WT mice (>8-fold, high-dose/low-dose) than in the *Cyp2a5*-null mice (<4-fold); this result is consistent with a more efficient clearance in the WT mice than in the *Cyp2a5*-null mice, at the low dose.

The formation and clearance of cotinine, the main circulating metabolite of nicotine, were also monitored in nicotine-treated mice. The AUC and C_{max} values for cotinine were much higher (>24-fold and >6-fold, respectively) than the corresponding values for nicotine, in WT

mice treated at either nicotine dose (Table 2). In nicotine-treated *Cyp2a5*-null mice, the rates of formation of cotinine appeared to be substantially lower, as indicated by lower C_{max} values, and higher T_{max} values, as compared to the values for the corresponding WT groups. However, rates of cotinine clearance also appeared to be lower, as reflected by significantly higher $t_{1/2}$ values.

The lower rate of cotinine clearance, as a result of the *Cyp2a5* deletion, was confirmed by additional studies in which circulating levels of cotinine were determined for cotinine-treated WT and *Cyp2a5*–null mice (Fig. 2C). As shown in Table 3, the rate of cotinine clearance was significantly lower (by 74% in CL/F value), whereas the AUC (by 3.7-fold) and $t_{1/2}$ (by 2-4-fold) values were higher, in the *Cyp2a5*-null mice than in the WT mice, at a cotinine dose of 1 mg/kg. Interestingly, in cotinine-treated mice, the lower rates of cotinine clearance in the *Cyp2a5*-null mice were accompanied by only marginally higher (1.3-fold; $p > 0.05$) cotinine C_{max} values, as compared to values for WT mice; this result can be explained by the much slower rate of first-pass metabolism of cotinine, as compared to metabolism of nicotine, in the liver.

For determination of the role of CYP2A5 in the regulation of tissue levels of nicotine and cotinine, a pharmacokinetic study was also carried out for liver, the main metabolic organ, and for brain, the target organ, with nicotine administered at 1 mg/kg. As shown in Figures 2, panels D and E, the concentration-time curves for tissue nicotine and cotinine levels were similar between the two organs, and also respectively similar to the curves determined for circulating nicotine and cotinine levels: much higher levels of nicotine, and much lower levels of cotinine, were seen in both liver and brain of the *Cyp2a5*-null mice than in liver and brain of the WT mice, at multiple time points after dosing. A further examination of the pharmacokinetic parameters for tissue nicotine and cotinine (Table 4) confirmed that CYP2A5 has a major impact on the bioavailability of nicotine and cotinine in the brain and the liver. In the *Cyp2a5*-null mice, the tissue levels of nicotine were higher in both liver (2.3-fold higher AUC, 1.2-fold higher C_{max})

JPET Fast Forward. Published on November 18, 2009 as DOI: 10.1124/jpet.109.162610
This article has not been copyedited and formatted. The final version may differ from this version.

and brain (2.7-fold higher AUC, 2.0-fold higher C_{max}), whereas tissue levels of cotinine were lower in both organs (>75% lower C_{max}, and 20-30% lower AUC), as compared to the levels for WT mice (Table 4).

Overall, the CYP2A5-associated pharmacokinetic changes for tissue nicotine and cotinine (Table 4) are similar to the changes seen in plasma (Table 2), and they are also comparable between brain and liver. This pattern is consistent with the notion that the impact of CYP2A5 is on systemic clearance, rather than on tissue distribution. In that context, the cotinine/nicotine abundance ratios were much higher for plasma than for liver and brain, in either WT or *Cyp2a5*-null mice; however, the abundance ratios were uniformly decreased in the *Cyp2a5*-null mice (Supplemental Table 3). Notably, tissue nicotine and cotinine levels were found to differ somewhat between brains and livers: AUC and C_{max} values for both nicotine and cotinine were higher in the liver than in the brain, for either mouse strain (Table 4). This tissue difference can be explained partly by the fact that the liver is the portal-of-entry organ for intraperitoneally injected nicotine, and by the fact that the bulk of the cotinine was produced in the liver.

Interestingly, at a nicotine dose of 1 mg/kg, the tissue/plasma abundance ratios for nicotine were higher in the WT mice than in the *Cyp2a5*-null mice, whereas the ratios for cotinine were similar between the WT and *Cyp2a5*-null mice (Supplemental Table 4). The lower tissue/plasma abundance ratios for nicotine, but not for cotinine, in the *Cyp2a5*-null mice can likely be explained by a saturation of tissue binding for nicotine, but not for cotinine, given the fact that tissue levels of nicotine (but not the levels of cotinine) were much higher in the null mice, than in the WT mice.

The lower rates of nicotine clearance in the *Cyp2a5*-null mice were likely due to the loss of CYP2A5-mediated cotinine formation in the liver; that notion is supported by results from in

vitro studies using hepatic microsomes from WT and *Cyp2a5*-null mice. Cotinine, formed through nicotine C-5'-oxidation (Fig. 3), is the major metabolite of nicotine in mouse hepatic microsomal reactions, as indicated by the relative abundances of all metabolites detected by LC-UV at 254 nm (data not shown). The conversion of the reactive intermediate to the stable cotinine was aided by the inclusion of aldehyde oxidase (contained in liver cytosol) (Beedham et al., 1987). As shown in Table 5, the rates of cotinine formation were 85% and 73% lower for hepatic microsomes from the *Cyp2a5*-null mice than for hepatic microsomes from WT mice, at respective nicotine concentrations of 1 and 10 μM. Notably, the CYP2A5 contribution to microsomal nicotine metabolism in the WT mice was greater at the lower substrate concentration (1 μM), a result further supporting the proposal that CYP2A5 is the low-Km enzyme in metabolizing nicotine.

We detected two other nicotine metabolites in mouse hepatic microsomal reaction mixtures (Fig. 3). One, which was detected only when KCN was included in the reaction mixture, was identified as a cyanide adduct (*m/z* = 188), given the characteristic neutral loss of an HCN motif (*m/z* = 27), and the features of other fragment ions in the product ion spectrum of the metabolite (not shown). The formation of the cyanide adduct indicated the presence of an iminium ion intermediate, which we propose to be the dihydropyrolium ion that is formed via the initial CYP2A5-mediated 5'-hydroxylation of nicotine (Fig. 3). The other metabolite (*m/z* = 149) had a mass fragmentation pattern consistent with that of nornicotine, which is formed from nicotine *N*-demethylation; notably, this metabolite does not represent a contaminant, given that it was not detected in zero-minute incubations. The roles of CYP2A5 in the formation of these apparently less abundant metabolites were not determined.

Discussion

The in vivo role of CYP2A5 in nicotine and cotinine clearance has recently been studied by others, who made use of either CYP2A5 chemical inhibitors (Raunio et al., 2008b), or mouse strains (B6 and DBA/2) that have allelic differences in the structure and function of the CYP2A5 protein (Siu and Tyndale, 2007). Pharmacokinetic parameters for plasma nicotine and cotinine were determined both in the study by Siu and Tyndale (2007) and in the present study; therefore, it is tempting to compare the results from these two studies. However, although B6 WT mice were treated with nicotine and cotinine (both at 1 mg/kg) in both studies, the experiments that correspond between the two studies in terms of compound and dose did not yield fully comparable results, given that the compounds were administered subcutaneously in the earlier study, but i.p. in ours. An examination of the pharmacokinetics data from the two studies indicates a difference in clearance rate, e.g., with the CL/F, AUC, and C_{max} values for nicotine being 5.2 ± 0.2 ml/min, 80.8 ± 3.2 ng*h/ml, and 160 ± 15 ng/ml, respectively, following s.c. injection (their study), and 31.9 ± 2.5 ml/min, 12.7 ± 0.5 ng*h/ml, and 43.2 ± 7.9 ng/ml, respectively, following i.p. injection (our study). This difference in clearance rates can be explained by the essential role of hepatic P450 enzymes in nicotine clearance and the differing proportions of the injected dose that are subjected to hepatic first-pass metabolism. While essentially all of the i.p.-injected dose of nicotine would be subjected to first-pass metabolism in the liver, before appearing in the systemic circulation, only a proportion of the s.c.-injected dose of nicotine would be distributed to the liver in each pass.

The study design of Siu and Tyndale (2007) also differed from that of the present study, in that total (conjugated and unconjugated) nicotine and cotinine were determined there, but only unconjugated compounds were determined here. The extent of glucuronidation of nicotine or cotinine in mice is not known (Siu and Tyndale, 2007). In earlier work, UGT activities toward

nicotine and cotinine had not been detected in mouse liver microsomes in vitro (Ghosheh and Hawes 2002). Therefore, it is unlikely that the use or non-use of a de-conjugation step, between these two pharmacokinetics studies, would have affected the experimental outcome to any large extent.

Interestingly, despite the difference in the route of injection (s.c. vs i.p.) between the two studies, and the large differences in pharmacokinetic parameters seen for nicotine clearance, essentially identical pharmacokinetic parameters were seen for cotinine clearance (after comparable cotinine injections at 1 mg/kg to WT B6 mice) in the two studies. This apparent independence on the injection route, for cotinine clearance, is consistent with a rate of hepatic cotinine metabolism that is much lower than the rate of hepatic nicotine metabolism (as was shown by Siu and Tyndale, 2007). Although the high-affinity Km values for B6 hepatic microsomal metabolism of nicotine and cotinine were similar (11.4 and 9.5 μM, respectively), the Vmax values differed by >10-fold (0.50 and 0.04 nmol/min/mg). Thus, a much smaller proportion of the dose will be removed through first-pass clearance for i.p.-injected cotinine than for i.p.-injected nicotine; conversely, given the overall differences in clearance rate (slower for cotinine than for nicotine), the majority of s.c.-injected cotinine will eventually have a chance to pass through liver, and be metabolized by hepatic CYP2A5.

The lower rate of nicotine clearance in the *Cyp2a5*-null mice was accompanied by a lower level of cotinine formation, as compared to the values for WT mice. Notably, the impact of the *Cyp2a5* deletion on nicotine AUC values (2.7-fold to 6.1-fold increases, null vs WT), and the impact of the *Cyp2a5* deletion on cotinine C_{max} values (56-67% reductions), an impact that mainly reflects the lower rate of nicotine metabolism, were more robust than was the impact on cotinine AUC values (18-35% reductions); the latter can be influenced by both rates of cotinine formation and rates of cotinine metabolism, in nicotine-teated mice. These findings relating to

the effects of the *Cyp2a5* gene deletion on pharmacokinetics of circulating nicotine and cotinine may aid in the interpretation of smoke exposure bio-monitoring results for individuals with genetic polymorphisms in the orthologous *CYP2A6* gene. In that regard, the dependence of serum cotinine levels on rates of both formation and elimination has been found previously in human smokers (Pérez-Stable et al., 1998).

Human CYP2A6 is less efficient than is CYP2A5 in the metabolism of nicotine; heterologously expressed CYP2A6 was found to have a Km value of 144 μM and a Vmax/Km value of 0.01 in nicotine C-5'-oxidation, whereas heterologously expressed CYP2A5 had a Km value of 7.7 μM and a Vmax/Km value of 0.20 (Murphy et al., 2005). In liver microsomes from WT B6 mice, a high-affinity component (Km 11.4 μM) and a low affinity component (Km 306 μM) were identified, with CYP2A5 being apparently responsible for the high-affinity site (Siu and Tyndale, 2007). Thus, in terms of the pharmacokinetics of nicotine clearance, the *Cyp2a5*-null mouse more closely resembles humans than does the WT B6 mouse. The residual activities toward nicotine in the *Cyp2a5*-null mice are likely contributed by other P450 enzymes that have either low affinity or low efficiency for this reaction, particularly members of the mouse *Cyp2b* subfamily (Siu and Tyndale, 2007). In this context, human CYP2B6 and rat CYP2B1/2 have been found to be active in nicotine 5'-oxidation (Nakayama et al., 1993; Schoedel et al., 2001; Yamazaki et al., 1999). Efforts are underway to prepare a CYP2A6-humanized mouse model, to enable direct study of CYP2A6-mediated nicotine metabolism in vivo.

It is important that we understand the impact of systemic metabolism on tissue levels of nicotine and cotinine in the brain, the pharmacological target organ for nicotine. Although cotinine does not have the same drug action as does nicotine, it does have the potential to modulate nicotine action, through its binding to epibatidine-sensitive nicotinic receptors (Vainio and Tuominen, 2001). Our observation of much higher (assuming that 1 g tissue is equivalent to

1 ml plasma) brain tissue levels than plasma levels, for nicotine, most likely reflects the higher tissue binding of nicotine in brain, as compared to plasma. In contrast, cotinine levels in the brain were actually slightly lower than levels in the plasma, of nicotine-treated mice. This finding may be explained by the slow rate of cotinine metabolism (relative to the rate of nicotine metabolism) in the liver; it may also reflect rate limitations for penetration of the blood-brain barrier by cotinine (Riah et al., 1998). Our findings concerning the effects of the *Cyp2a5* gene deletion on nicotine and cotinine levels, and on the cotinine/nicotine abundance ratios, in the brains and plasma of nicotine-treated mice, should be taken into account, when predictions are made, on the basis of the measurable plasma levels, for brain levels of nicotine and cotinine, in nicotine-exposed individuals.

The neuroprotective effects of nicotine against chemically induced neurotoxicity have been consistently demonstrated in experimental rat and monkey models, but conflicting results have been found in mice (Quik et al., 2007). Nicotine clearance is much faster in mice than in humans, monkeys, and rats; it is conceivable that we are not able to maintain adequate levels of nicotine in the mouse brain for a sufficiently long period to enable effective neuroprotection, particularly for chronic effects involving nicotine-induced alterations in gene expression. Our finding, that plasma nicotine $t_{1/2}$ values, as well as brain nicotine levels, are significantly higher in nicotine-treated *Cyp2a5*-null mice than in the similarly dosed WT mice, suggests that the *Cyp2a5*-null mouse model is valuable for efforts to establish whether effective neuroprotection by nicotine can be achieved in mouse models through suppression of systemic clearance.

In summary, several features of our *Cyp2a5*-null mouse make it a suitable model for applications in drug metabolism and toxicology research. These features include the B6 genetic background; the specific deletion of the single mouse *Cyp2a* gene (sparing *Cyp2a4* and *Cyp2a12*); the absence of a negative effect of the *Cyp2a5* disruption on the expression of

neighboring *Cyp2a12*, *Cyp2g1*, and *Cyp2b* genes; the absence of compensatory changes in the expression of other biotransformation enzymes examined; and the lack of any concomitant reproductive or developmental defects. In a first application of the *Cyp2a5*-null model to in vivo drug metabolism studies, we have examined the role of CYP2A5 in systemic clearance of nicotine and cotinine. Our findings provided direct evidence that CYP2A5 plays an essential role in the in vivo metabolism of both nicotine and cotinine. Our pharmacokinetic analysis of plasma and tissue nicotine and cotinine levels in the *Cyp2a5*-null mice should have important implications for an understanding of the impact of genetic polymorphisms in the *CYP2A6* gene on pharmacokinetics of nicotine and cotinine in human brain and plasma. In addition, future studies on the efficacy of nicotine as a neuroprotective agent in the *Cyp2a5*-null mouse model are warranted.

Acknowledgements

We are grateful to Drs. Ming Yao and Mingshe Zhu of the Department of Biotransformation, Bristol-Myers Squibb, Princeton, NJ, for helpful discussions. We acknowledge the use of the Transgenic and Knockout Mouse Core, and the Biochemistry Core, of the Wadsworth Center. We thank Dr. Adriana Verschoor of the Wadsworth Center, Dr. Sharon Murphy of the University of Minnesota, and Dr. Rachel Tyndale of the University of Toronto, for comments on the manuscript; Dr. Kenneth Aldous for advice on LC/MS analysis of nicotine and cotinine; and Ms. Weizhu Yang for technical assistance.

References

Beedham C (1987) Molybdenum hydroxylases: biological distribution and substrate-inhibitor specificity. *Prog Med Chem* **24**:85-127.

Benowitz NL, Swan GE, Jacob P, III, Lessov-Schlaggar CN, and Tyndale RF (2006) CYP2A6 genotype and the metabolism and disposition kinetics of nicotine. *Clin Pharmacol Ther* **80**:457-467.

Cashman JR (2000) Human flavin-containing monooxygenase: substrate specificity and role in drug metabolism. *Curr Drug Metab* **1**:181-191.

Cashman JR, Park SB, Yang ZC, Wrighton SA, Jacob P, III, and Benowitz NL (1992) Metabolism of nicotine by human liver microsomes: stereoselective formation of trans-nicotine N'-oxide. *Chem Res Toxicol* **5**:639-646.

de Leon J, Diaz FJ, Rogers T, Browne D, Dinsmore L, Ghosheh OH, Dwoskin LP, and Crooks PA (2002) Total cotinine in plasma: a stable biomarker for exposure to tobacco smoke. *J Clin Psychopharmacol* **22**:496-501.

Ding X and Coon MJ (1988), Purification and characterization of two unique forms of cytochrome P-450 from rabbit nasal microsomes. *Biochemistry* 27:8330-8337.

Ding X and Coon MJ (1990) Immunochemical characterization of multiple forms of cytochrome P-450 in rabbit nasal microsomes and evidence for tissue-specific expression of P-450s NMa and NMb. *Mol Pharmacol* **37**:489-496.

Ding X and Coon MJ (1994), Steroid metabolism by rabbit olfactory-specific P450 2G1. *Arch Biochem Biophys* 315:454-459.

Ghosheh O and Hawes EM (2002) Microsomal N-glucuronidation of nicotine and cotinine: human hepatic interindividual, human intertissue, and interspecies hepatic variation. *Drug Metab Dispos* **30**:1478-1483.

Heavner DL, Richardson JD, Morgan WT, and Ogden MW (2005) Validation and application of a method for the determination of nicotine and five major metabolites in smokers' urine by solid-phase extraction and liquid chromatography-tandem mass spectrometry. *Biomed Chromatogr* **19**:312-328.

Hukkanen J, Jacob P, III, and Benowitz NL (2005) Metabolism and disposition kinetics of nicotine. *Pharmacol Rev* **57**:79-115.

Kaivosaari S, Toivonen P, Hesse LM, Koskinen M, Court MH, and Finel M (2007) Nicotine Glucuronidation and the Human UDP-Glucuronosyltransferase UGT2B10. *Mol Pharmacol* **72**:761-768.

Kontgen F, Suss G, Stewart C, Steinmetz M, and Bluethmann H (1993) Targeted disruption of the MHC class II Aa gene in C57BL/6 mice. *Int Immunol* **5**:957-964.

Kuehl GE and Murphy SE (2003) N-glucuronidation of nicotine and cotinine by human liver microsomes and heterologously expressed UDP-glucuronosyltransferases. *Drug Metab Dispos* **31**:1361-1368.

Messina ES, Tyndale RF, and Sellers EM (1997) A major role for CYP2A6 in nicotine C-oxidation by human liver microsomes. *J Pharmacol Exp Ther* **282**:1608-1614.

Murphy SE, Raulinaitis V, and Brown KM (2005) Nicotine 5'-oxidation and methyl oxidation by P450 2A enzymes. *Drug Metab Dispos* **33**:1166-1173.

Nakajima M, Yamamoto T, Nunoya K, Yokoi T, Nagashima K, Inoue K, Funae Y, Shimada N, Kamataki T, and Kuroiwa Y (1996) Role of human cytochrome P4502A6 in C-oxidation of nicotine. *Drug Metab Dispos* **24**:1212-1217.

Nakayama H, Okuda H, Nakashima T, Imaoka S, and Funae Y (1993) Nicotine metabolism by rat hepatic cytochrome P450s. *Biochem Pharmacol* **45**:2554-2556.

Pérez-Stable EJ, Herrera B, Jacob P 3rd, Benowitz NL (1998) Nicotine metabolism and intake in black and white smokers. *JAMA* **280**:152-156.

Quik M, O'Neill M, and Perez XA (2007) Nicotine neuroprotection against nigrostriatal damage: importance of the animal model. *Trends Pharmacol Sci* **28**:229-235.

Raunio H, Hakkola J and Pelkonen O (2008a) The CYP2A subfamily in Cytochrome P450 role in metabolism and toxicity of drugs and other xenobiotics (Ioannides C ed) pp 151–171, Advancing the Chemical Sciences Publishing, Cambridge, UK.

Raunio H, Pokela N, Puhakainen K, Rahnasto M, Mauriala T, Auriola S, and Juvonen RO (2008b) Nicotine metabolism and urinary elimination in mouse: in vitro and in vivo. *Xenobiotica* **38**:34-47.

Ravina BM, Fagan SC, Hart RG, Hovinga CA, Murphy DD, Dawson TM, and Marler JR (2003) Neuroprotective agents for clinical trials in Parkinson's disease: a systematic assessment. *Neurology* **60**:1234-1240.

Riah O, Courriere P, Dousset JC, Todeschi N, and Labat C (1998) Nicotine is more efficient than cotinine at passing the blood-brain barrier in rats. *Cell Mol Neurobiol* **18**:311-318.

Schoedel KA, Sellers EM, and Tyndale RF (2001) Induction of CYP2B1/2 and nicotine metabolism by ethanol in rat liver but not rat brain. *Biochem Pharmacol* **62**:1025–1036.

Siu EC and Tyndale RF (2007) Characterization and comparison of nicotine and cotinine metabolism in vitro and in vivo in DBA/2 and C57BL/6 mice. *Mol Pharmacol* **71**:826-834.

Siu EC, Wildenauer DB, and Tyndale RF (2006) Nicotine self-administration in mice is associated with rates of nicotine inactivation by CYP2A5. *Psychopharmacology (Berl)* **184**:401-408.

Statler PA, McPherson RJ, Bauer LA, Kellert BA, and Juul SE (2007) Pharmacokinetics of high-dose recombinant erythropoietin in plasma and brain of neonatal rats. *Pediatr Res* **61**:671-675.

Su T and Ding X (2004) Regulation of the cytochrome P450 2A genes. *Toxicol Appl Pharmacol* **199**:285-294.

Tai SS, Xu B, and Welch MJ (2006) Development and evaluation of a candidate reference measurement procedure for the determination of progesterone in human serum using isotope-dilution liquid chromatography/tandem mass spectrometry. *Anal Chem* **78**:6628-6633.

Vainio PJ and Tuominen RK (2001) Cotinine binding to nicotinic acetylcholine receptors in bovine chromaffin cell and rat brain membranes. *Nicotine Tob Res* **3**:177-182.

Wang H, Donley KM, Keeney DS, and Hoffman SM (2003) Organization and evolution of the Cyp2 gene cluster on mouse chromosome 7, and comparison with the syntenic human cluster. *Environ Health Perspect* **111**:1835-1842.

Wong G, Kawajiri K, and Negishi M (1987) Gene family of male-specific testosterone 16 alpha-hydroxylase (C-P-450(16) alpha) in mouse liver: cDNA sequences, neonatal imprinting, and reversible regulation by androgen. *Biochemistry* **26**:8683-8690.

Wong HL, Murphy SE, Hecht SS (2005) Cytochrome P450 2A-catalyzed metabolic activation of structurally similar carcinogenic nitrosamines: N'-nitrosonornicotine enantiomers, N-nitrosopiperidine, and N-nitrosopyrrolidine. *Chem Res Toxicol* **18**: 61-69.

Yanagimoto T, Itoh S, Muller-Enoch D, Kamataki T. (1992) Mouse liver cytochrome P-450 (P-450IIIAM1): its cDNA cloning and inducibility by dexamethasone. *Biochim Biophys Acta* 1130:329-332.

Yamazaki H, Inoue K, Hashimoto M, and Shimada T (1999) Roles of CYP2A6 and CYP2B6 in nicotine C-oxidation by human liver microsomes. *Arch Toxicol* **73**:65–70.

Zhang X, Zhang Q-Y, Liu D, Su T, Weng Y, Ling G, Chen Y, Gu J, Schilling B, and Ding X (2005) Expression of cytochrome p450 and other biotransformation genes in fetal and adult human nasal mucosa. *Drug Metab Dispos* **33**:1423-1428.

Zhou X, Zhang X, Weng Y, Fang C and Ding X (2009) High abundance of testosterone and salivary androgen-binding protein in the lateral nasal gland of male mice. *J Steroid Biochem Mol Biol* in press.

Zhuo X, Gu J, Behr MJ, Swiatek PJ, Cui H, Zhang QY, Xie Y, Collins DN, and Ding X (2004) Targeted disruption of the olfactory mucosa-specific *Cyp2g1* gene: impact on acetaminophen toxicity in the lateral nasal gland, and tissue-selective effects on Cyp2a5 expression. *J Pharmacol Exp Ther* **308**:719-728.

Footnotes

This work was supported in part by the National Institutes of Health National Cancer Institute [Grant CA092596] and the National Institutes of Health National Institute of Environmental Health Sciences [Grant ES007462].

Legends for Figures

Fig. 1. Targeted disruption of the mouse *Cyp2a5* gene

Structures of the WT *Cyp2a5* allele and the *Cyp2a4*/*Cyp2a12* allele (A), the targeting vector (B), and the targeted allele (C) are depicted. Both external (Probe E) and internal (Probe I) probes were used for Southern blot analysis. The restriction site PvuII (P) was used to distinguish between *Cyp2a4*/*Cyp2a12* and *Cyp2a5* WT alleles. D, detection of the targeted *Cyp2a5* allele by Southern blot analysis of mouse tail genomic DNA. The 7.0-kb, 4.0-kb, and 2.0-kb bands (detected with Probe E) represent the WT *Cyp*2a5 allele (+), targeted *Cyp*2a5 allele (-), and WT *Cyp2a4*/*Cyp2a12* alleles, respectively. E, absence of full-length or truncated CYP2A5 mRNA in tissues of the *Cyp2a5*-null mice. RNA-PCR was carried out as described in *Materials and Methods*. E2_E3 and E8_E9 respectively represent primer sets flanking exons 2 and 3, and sets flanking exons 8 and 9.

Fig. 2. Systemic and tissue levels of nicotine and cotinine at various time points after intraperitoneal administration of nicotine or cotinine

WT and *Cyp2a5*-null mice (2-month-old, male) were injected with nicotine or cotinine at the indicated dose, and levels of nicotine and/or cotinine were determined in the plasma, liver, and brain, at various time points after the injection. Body weights were not different between the two mouse strains. A and B, Plasma levels of nicotine and cotinine after an i.p. injection of nicotine at 1 mg/kg (A) or 5 mg/kg (B); C, Plasma levels of cotinine after an i.p. injection of cotinine at 1 mg/kg; D and E, levels of nicotine and cotinine in the liver (D) and brain (E) after an i.p. injection of nicotine at 1 mg/kg. Data represent means ± S.D. (n = 4-5, for plasma, or n = 3-4, for tissue). **, $P < 0.01$, compared with levels in WT mice.

Fig. 3. Identification of nicotine metabolites produced in mouse liver microsomal reactions

The reaction mixtures contained 50 mM potassium phosphate buffer, pH 7.4, 10 μM nicotine, 1.0 mg/ml liver microsomal protein from 2-month-old male WT mice, and 1.0 mM NADPH, with or without 10 mM KCN. Metabolite analysis was carried out with a LCQ Deca-XP LC/MS instrument, as described in *Materials and Methods*. Three metabolites (cotinine, nornicotine, and a cyanide-adduct of nicotine) were identified; their structures and fragmentation patterns, as well as the metabolic pathways that led to their formation, are shown.

JPET Fast Forward. Published on November 18, 2009 as DOI: 10.1124/jpet.109.162610
This article has not been copyedited and formatted. The final version may differ from this version.

Table 1. In vitro metabolism of testosterone by liver microsomes of WT and *Cyp2a5*-null mice

Rates of formation of three major testosterone metabolites, 15β-hydroxy-testosterone (15β-OH-T), 16α-OH-T, and 6β-OH-T, were determined. Reaction mixtures contained 50 mM potassium phosphate buffer, pH 7.4, 5.0 or 10 μM testosterone, 1.0 mM ascorbic acid, 0.1 mg/ml liver microsomal protein from 2-month-old male mice, and 1.0 mM NADPH. The values presented are means ± S.D. (n = 3).

Testosterone concentration	Genotype	Rates of product formation		
		15β-OH-T	16α-OH-T	6β-OH-T
		pmol/min/mg protein		
5 *μM*	WT	4.6 ± 1.1	240 ± 50	100 ± 30
	Cyp2a5-null	2.3 ± 0.1[a]	250 ± 30	100 ± 20
10 *μM*	WT	6.1 ± 0.7	270 ± 30	130 ± 20
	Cyp2a5-null	2.9 ± 0.5[a]	280 ± 50	140 ± 20

[a] Significantly lower than the corresponding WT value ($P < 0.05$)

JPET Fast Forward. Published on November 18, 2009 as DOI: 10.1124/jpet.109.162610
This article has not been copyedited and formatted. The final version may differ from this version.

Table 2. Pharmacokinetic parameters for plasma nicotine and cotinine, in mice treated with nicotine

Mice were given nicotine (i.p.) at either 1 or 5 mg/kg. Values were derived from plots shown in Figure 2, panels A and B. Results shown represent means ± S.D. (n = 4-5).

Nicotine dose (mg/kg)	Analyte	Mouse strain	$AUC_{0\text{-}240\ min}$ (ng·h/ml)	$t_{1/2}$ (min)	CL/F (ml/min)	T_{max} (min)	C_{max} (ng/ml)
1	Nicotine	WT	12.7 ± 0.5	12.9 ± 3.2	31.9 ± 2.5	5.0 ± 0.0	43.2 ± 7.9
		Cyp2a5-null	77.3 ± 8.2[a]	35.5 ± 2.9[a]	5.72 ± 0.60[a]	5.0 ± 0.0	139 ± 38[a]
	Cotinine	WT	391 ± 50	38.2 ± 2.7	N/A[b]	16.3 ± 10.3	267 ± 55
		Cyp2a5-null	253 ± 25[a]	119 ± 43[a]	N/A	52.5 ± 22.0[a]	89.2 ± 11.0[a]
5	Nicotine	WT	107 ± 21	70.5 ± 15.0	25.3 ± 4.1	5.0 ± 0.0	113 ± 36
		Cyp2a5-null	292 ± 61[a]	95.9 ± 14.0[c]	7.49 ± 2.50[a]	5.0 ± 0.0	385 ± 105[c]
	Cotinine	WT	2600 ± 340	55.0 ± 9.4	N/A	52.5 ± 15.0	1010 ± 80
		Cyp2a5-null	2140 ± 210	167 ± 47[a]	N/A	90.0 ± 35.0	449 ± 56[a]

[a] $P < 0.01$, compared with corresponding WT value

[b] N/A, not applicable

[c] $P < 0.05$, compared with corresponding WT value

Table 3. Pharmacokinetic parameters for plasma cotinine, in mice treated with cotinine

Mice were injected with cotinine at 1 mg/kg (i.p.). Values were derived from plots shown in Figure 2C. Results shown represent means ± S.D. (n = 4).

Strain	$AUC_{0\text{-}480\ min}$ (ng·h/ml)	$t_{1/2}$ (min)	CL/F (ml/min)	T_{max} (min)	C_{max} (ng/ml)
WT	847 ± 95	54.6 ± 3.1	0.43 ± 0.01	15.0 ± 0.0	627 ± 76
Cyp2a5-null	3140 ± 240[a]	131 ± 19[a]	0.11 ± 0.02[a]	22.5 ± 8.6	827 ± 136

[a] $P < 0.01$, compared with corresponding WT value

JPET Fast Forward. Published on November 18, 2009 as DOI: 10.1124/jpet.109.162610
This article has not been copyedited and formatted. The final version may differ from this version.

Table 4. Pharmacokinetic parameters for tissue nicotine and cotinine levels, in mice treated with nicotine

Mice were given nicotine (i.p.) at 1 mg/kg. Values were derived from plots shown in Figure 2, panels D and E. Pharmacokinetic parameters were calculated using mean concentration values (n = 3-4) for each time point; each mouse was used for a single time point.

Tissue	Analyte	Strain	$AUC_{0\text{-}240\ min}$ (ng·h/g)	$t_{1/2}$ (min)	T_{max} (min)	C_{max} (ng/g)
Brain	Nicotine	WT	98.9	46.3	5.0	233
		Cyp2a5-null	263	44.8	5.0	477
	Cotinine	WT	219	37.8	15.0	218
		Cyp2a5-null	160	199	60.0	50.2
Liver	Nicotine	WT	157	32.4	5.0	658
		Cyp2a5-null	365	43.4	5.0	761
	Cotinine	WT	350	34.4	5.0	468
		Cyp2a5-null	275	149	30.0	109

JPET Fast Forward. Published on November 18, 2009 as DOI: 10.1124/jpet.109.162610
This article has not been copyedited and formatted. The final version may differ from this version.

Table 5. Rates of in vitro metabolism of nicotine by liver microsomes from WT and *Cyp2a5*-null mice

Cotinine formation was determined as described in *Materials and Methods*. Reaction mixtures contained 50 mM potassium phosphate buffer, pH 7.4, 1.0 or 10 μM nicotine, 0.5 mg/ml liver microsomal protein, and 1.0 mg/ml liver cytosol protein (as a source of aldehyde oxidase) from 2-month-old male mice, and 1.0 mM NADPH. The values presented are means ± S.D. (n = 3).

Nicotine concentration	Strain	Rates of cotinine formation *pmol/min/mg*	Ratio of Null/WT
1.0 μM	WT	39.1± 1.2	0.15
	Cyp2a5-null	5.7 ± 0.8[a]	
10 μM	WT	221 ± 2	0.27
	Cyp2a5-null	58.6 ± 3.8[a]	

[a] $P < 0.01$, compared with the corresponding WT value

JPET Fast Forward. Published on November 18, 2009 as DOI: 10.1124/jpet.109.162610
This article has not been copyedited and formatted. The final version may differ from this version.

Fig. 1

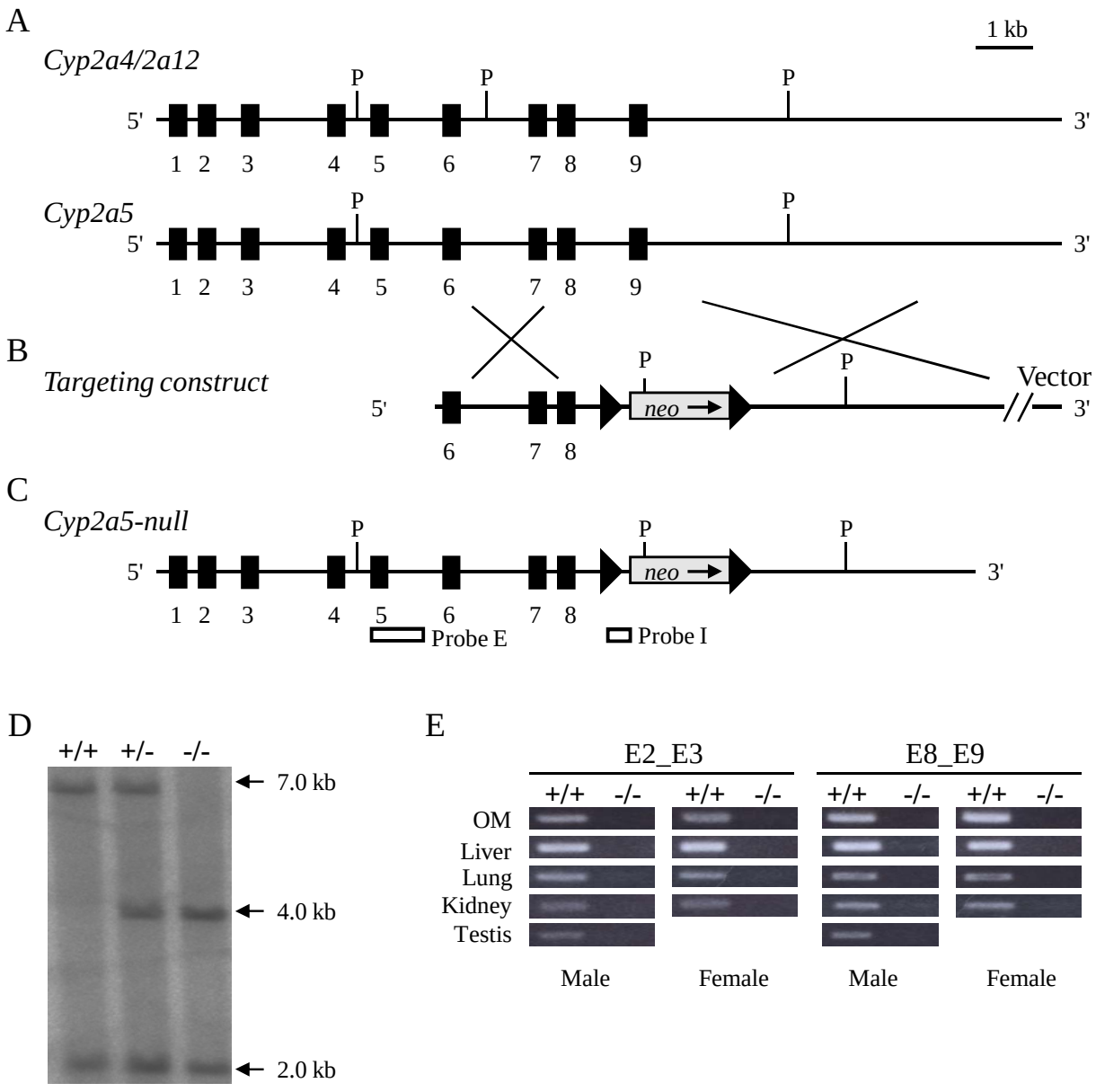

JPET Fast Forward. Published on November 18, 2009 as DOI: 10.1124/jpet.109.162610
This article has not been copyedited and formatted. The final version may differ from this version.

Fig. 2

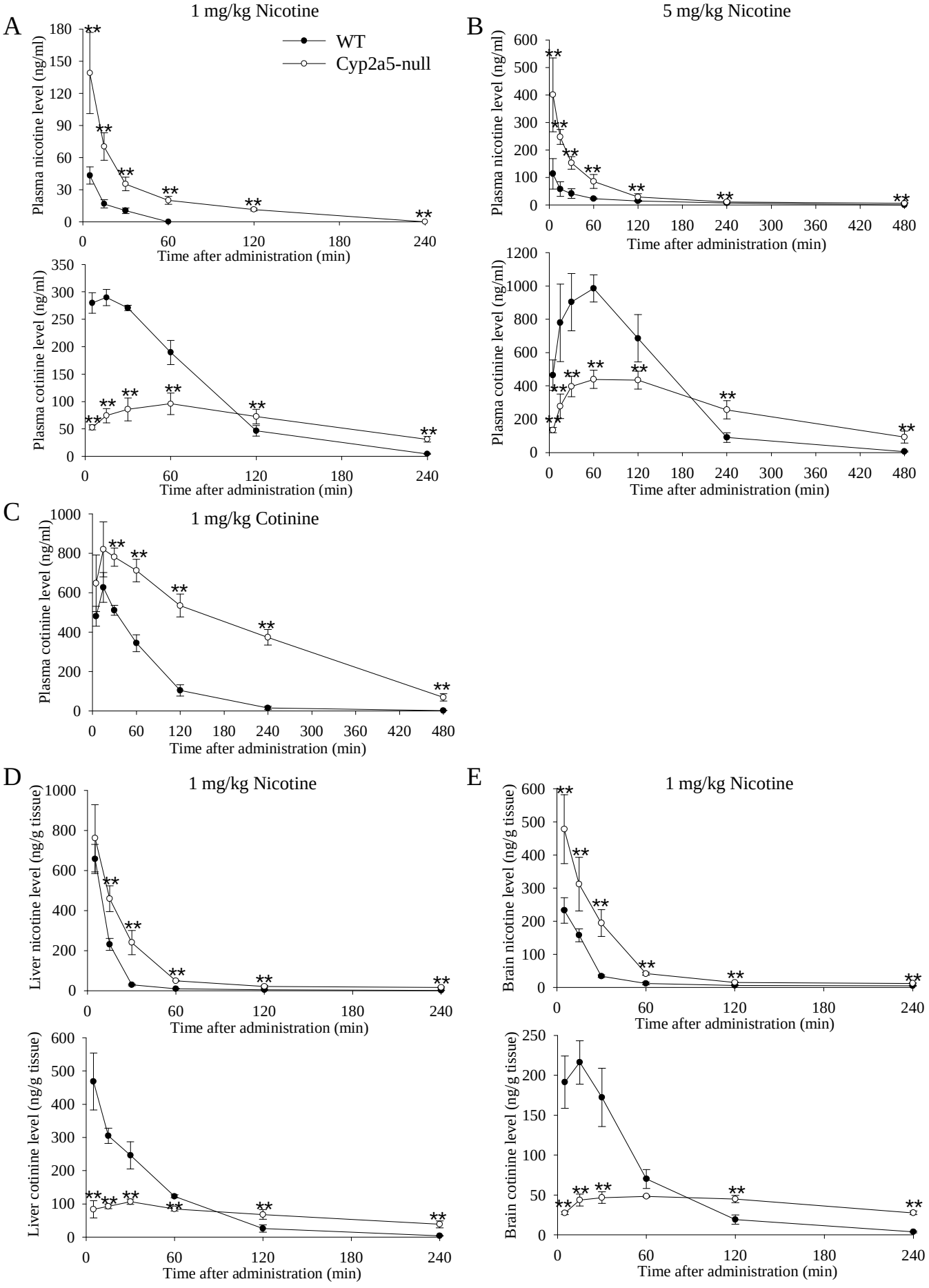

JPET Fast Forward. Published on November 18, 2009 as DOI: 10.1124/jpet.109.162610
This article has not been copyedited and formatted. The final version may differ from this version.

Fig.3

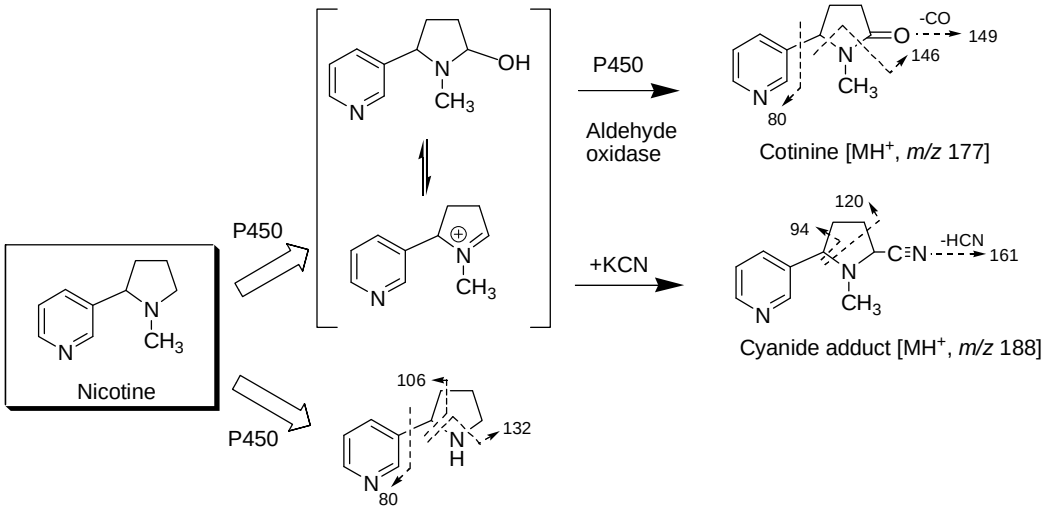

Role of CYP2A5 in the Clearance of Nicotine and Cotinine: Insights from Studies on a *Cyp2a5*-null Mouse Model

Xin Zhou, Xiaoliang Zhuo, Fang Xie, Kerri Kluetzman, Yue-Zhong Shu, W. Griffith Humphreys, and Xinxin Ding

Supplemental Materials

Additional Materials and Methods

Determination of CYP2G1 and CYP2A12 mRNA levels. Real-time RNA-PCR analysis was performed for olfactory mucosal CYP2G1 and hepatic CYP2A12, according to the general protocol described previously (Zhang et al., 2005), with use of an ABI 7500 Fast Real-Time PCR System and SYBR Green core reagents (Applied Biosystems, Foster City, CA). The primers used for real-time PCR for CYP2G1 and GAPDH were described previously (Gu et al., 1999). The primers for CYP2A12 quantification were 5'-ttgatcaagatgttgcaggg-3' and 5'-ttgcatgtggatgagaaagg-3' (according to Mouse Genome Informatics, the Jackson Lab, Bar Harbor, ME); the PCR was performed at an annealing temperature of 62°C. Based on sequence alignments, the primers for CYP2A12 can amplify both CYP2A12 and CYP2A22 cDNAs; however, sequence analysis of PCR products obtained from the liver indicated that CYP2A22 mRNA was absent (data not shown). PCR products were validated by sequence analysis, and PCR specificity was confirmed by analysis of reaction products on agarose gels. One of the samples was serially diluted for construction of a standard curve. The results were corrected on the basis of the levels of GAPDH mRNA present in the same RNA preparation.

Immunoblot analysis. The levels of P450 and UGTs were determined by immunoblot, using the following antibodies: goat anti-rat CYP2B1, goat anti-rat CYP3A2, rabbit anti-rat CPR, and rabbit anti-human CYP2C9/2C10 (BD Gentest, Woburn, MA); rabbit anti-human UGT1A1 and rabbit anti-human UGT2B4 (Santa Cruz, Santa Cruz, CA). Immunoblot analysis was carried out essentially as described previously (Ding and Coon, 1990). The intensity of the detected bands was quantified with a densitometer, as described previously (Zhuo et al., 2004).

Identification and quantitative analysis of testosterone metabolites. A 4-μm Nova-Pak C18 column (3.9 x 150 mm, Waters, Milford, MA) was used. The column was equilibrated with 85%A:15%B, and the samples were eluted using one of two solvent gradient systems, at a flow rate of 1 ml/min. In system one, the solvent gradient consisted linear increases from 15%B to 30%B between 3 and 25 min, and then from 30%B to 40%B between 25 and 26 min, followed by a 4-min wash with 100%B; the parent/product ion pairs of *m/z* 305/97 for 16α-OH-T) and 305/269 (for 6β-OH-T) were measured in the Multiple Reaction Monitoring (MRM) scan mode. In system two, the solvent gradient consisted linear increases from 15%B to 30%B between 2 and 60 min, and then from 30%B to 100%B between 60 and 61 min, followed by a 3-min wash with 100%B; the parent/product ion pairs of *m/z* 305/97 (for 15β-OH-T) was measured in the MRM scan mode.

Quantitative analysis of testosterone and progesterone. A LC/MS system consisting of an Agilent 1200 Series HPLC and an ABI 4000 Q-Trap mass spectrometer (Applied Biosystem), with a 4-μm Nova-Pak C18 column (3.9 x 150 mm, Waters, Milford, MA), was used. The mobile phase consisted of solvent A (0.1% formic acid in water/acetonitrile (95:5)) and solvent B (0.1% formic acid in water/acetonitrile (5:95)). The column was equilibrated with 60%A:40%B; the samples were eluted, at a flow rate of 0.5 ml/min, with 40% B for 2 min; followed by linear increases from 40%B to 100%B, between 2 and 8 min, and then by 100%B for 4 min. The retention time for progesterone (and the internal standard) was 11.2 min. The MS was operated in the positive ion mode, using atmospheric pressure chemical ionization. The parent/product ion pairs of *m/z* 315/97 and 315/109 (for progesterone), and *m/z* 317/99 and 317/111 (for 3,4-^{13}C-progesterone), were measured in the MRM scan mode. The parameters for

the chamber were: curtain gas, 30 psig; needle current, 5 μA; heated nebulizer temperature, 350°C; nebulizing gas, 50 psig; declustering potential, 80 V; and entrance potential, 5.0 V.

Supplemental References

Ding X and Coon MJ (1990) Immunochemical characterization of multiple forms of cytochrome P-450 in rabbit nasal microsomes and evidence for tissue-specific expression of P-450s NMa and NMb. *Mol Pharmacol* **37**:489-496.

Gu J, Dudley C, Su T, Spink DC, Zhang QY, Moss RL, and Ding X (1999) Cytochrome P450 and steroid hydroxylase activity in mouse olfactory and vomeronasal mucosa. *Biochem Biophys Res Commun* **266**:262-267.

Zhang X, Zhang Q-Y, Liu D, Su T, Weng Y, Ling G, Chen Y, Gu J, Schilling B, and Ding X (2005) Expression of cytochrome p450 and other biotransformation genes in fetal and adult human nasal mucosa. *Drug Metab Dispos* **33**:1423-1428.

Zhuo X, Gu J, Behr MJ, Swiatek PJ, Cui H, Zhang QY, Xie Y, Collins DN, and Ding X (2004) Targeted disruption of the olfactory mucosa-specific *Cyp2g1* gene: impact on acetaminophen toxicity in the lateral nasal gland, and tissue-selective effects on Cyp2a5 expression. *J Pharmacol Exp Ther* **308**:719-728.

Supplemental Table S1

Genotype distribution in pups derived from intercrosses between *Cyp2a5*$^{+/-}$ mice

	Number of pups in each genotype		
	Homozygous	Heterozygous	WT
Male	11	22	13
Female	10	24	11
Combined	21	46	24
Expected[a]	24	48	24

[a]The number of pups expected in each genotype was calculated by assuming Mendelian distribution for the WT littermates. No significant difference was found (P = 0.865, chi-square test)

Supplemental Table S2

Body and tissue weights of WT and *Cyp2a5*-null mice

The body weight and organ weights of male and female mice were determined at 2 months of age. Values reported are means ± S.D. (n = 8). There was no significant difference between WT and *Cyp2a5*-null (Null) mice (P > 0.05).

Genotype	Body weight (*g*)		Tissue weight (*g*)						
			Liver		Lung		Kidney		Testis
	Male	Female	Male	Female	Male	Female	Male	Female	Male
WT	24.6 ± 0.7	20.7 ± 1.5	1.42± 0.08	1.21 ± 0.06	0.15 ± 0.01	0.14 ± 0.01	0.37 ± 0.02	0.27 ± 0.03	0.18 ± 0.02
Null	23.8 ± 0.9	20.5 ± 0.8	1.36 ± 0.09	1.16 ± 0.08	0.15 ± 0.02	0.14 ± 0.01	0.35 ± 0.02	0.27 ± 0.01	0.17 ± 0.02

Supplemental Table S3

Cotinine/nicotine abundance ratios for plasma, liver, and brain of WT and *Cyp2a5*-null mice

The values were calculated from data in Tables 2 and 4, for mice treated at a nicotine dose of 1 mg/kg.

Strain	Cotinine/nicotine abundance ratios					
	Plasma		Liver		Brain	
	AUC	C_{max}	*AUC*	C_{max}	*AUC*	C_{max}
WT	31	6.2	2.2	0.71	2.2	0.94
Cyp2a5-null	3.3	0.64	0.75	0.14	0.61	0.11

Supplemental Table S4

Tissue/plasma abundance ratios for nicotine and cotinine in WT and *Cyp2a5*-null mice

The values were calculated from data in Tables 2 and 4, for mice treated at a nicotine dose of 1 mg/kg.

Analyte	Strain	Brain/plasma abundance ratios		Liver/plasma abundance ratios	
		AUC	C_{max}	*AUC*	C_{max}
Nicotine	WT	7.8	5.4	12.4	15.2
	Cyp2a5-null	3.4	3.4	4.7	5.5
Cotinine	WT	0.6	0.8	0.9	1.7
	Cyp2a5-null	0.6	0.6	1.1	1.2

Supplemental Figure Legends

Figure S1. Quantitative analysis of CYP2G1 mRNA level in the olfactory mucosa of WT and *Cyp2a5*-null mice. Total RNA from the olfactory mucosa (OM) of 2-month-old mice was used for real-time RNA-PCR analysis. The values shown represent means ± S.D. (n = 4). There was no significant difference between WT and *Cyp2a5*-null mice in CYP2G1 expression (P >0.3, for either male or female mice).

Figure S2. Absence of compensatory increases in the expression of selected P450 and UGT enzymes in the livers of the *Cyp2a5*-null mice. Liver microsomes (5 μg) were analyzed in duplicate on immunoblots. The antibodies used are described above in *Additional Materials and Methods*. Microsomes were prepared from pooled livers from three male mice (2-month-old). Densitometric analysis indicated that, in each panel, the maximal difference in band intensity between samples from different animal groups was less than 20%.

Figure S3. Serum and testosterone and progesterone levels in WT and *Cyp2a5*-null mice. (A). Serum testosterone levels in male mice. (B). Serum progesterone levels in female mice. Testosterone and progesterone levels were determined for 2-month-old male and female mice (n=8), respectively. The values shown are the medians, together with the 25% (lower bar) and 75% (upper bar) percentile marks. No significant difference was found, for testosterone or progesterone levels, between WT and *Cyp2a5*-null groups (Mann-Whitney Rank Sum Test).

Figure S1. Quantitative analysis of CYP2G1 mRNA level in the olfactory mucosa of WT and *Cyp2a5*-null mice. Total RNA from the olfactory mucosa (OM) of 2-month-old mice was used for real-time RNA-PCR analysis. The values shown represent means ± S.D. (n = 4). There was no significant difference between WT and *Cyp2a5*-null mice in CYP2G1 expression (P >0.3, for either male or female mice).

Fig. S1

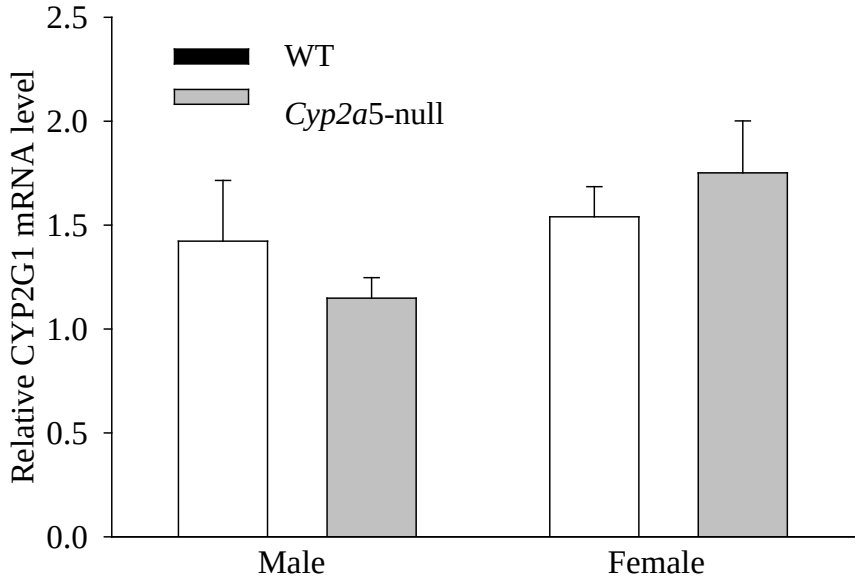

Fig. S2

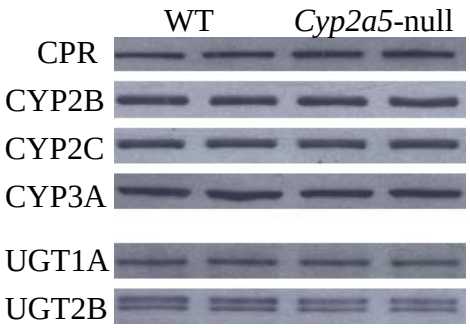

Figure S2. Absence of compensatory increases in the expression of selected P450 and UGT enzymes in the livers of the *Cyp2a5*-null mice. Liver microsomes (5 μg) were analyzed in duplicate on immunoblots. The antibodies used are described above in *Additional Materials and Methods*. Microsomes were prepared from pooled livers from three male mice (2-month-old). Densitometric analysis indicated that, in each panel, the maximal difference in band intensity between samples from different animal groups was less than 20%.

Figure S3. Serum and testosterone and progesterone levels in WT and *Cyp2a5*-null mice. (A). Serum testosterone levels i

Xin Zhou, Xiaoliang Zhuo, Fang Xie, Kerri Kluetzman, Yue-Zhong Shu, W. Griffith Humphreys, and Xinxin Ding*

Fig. S3

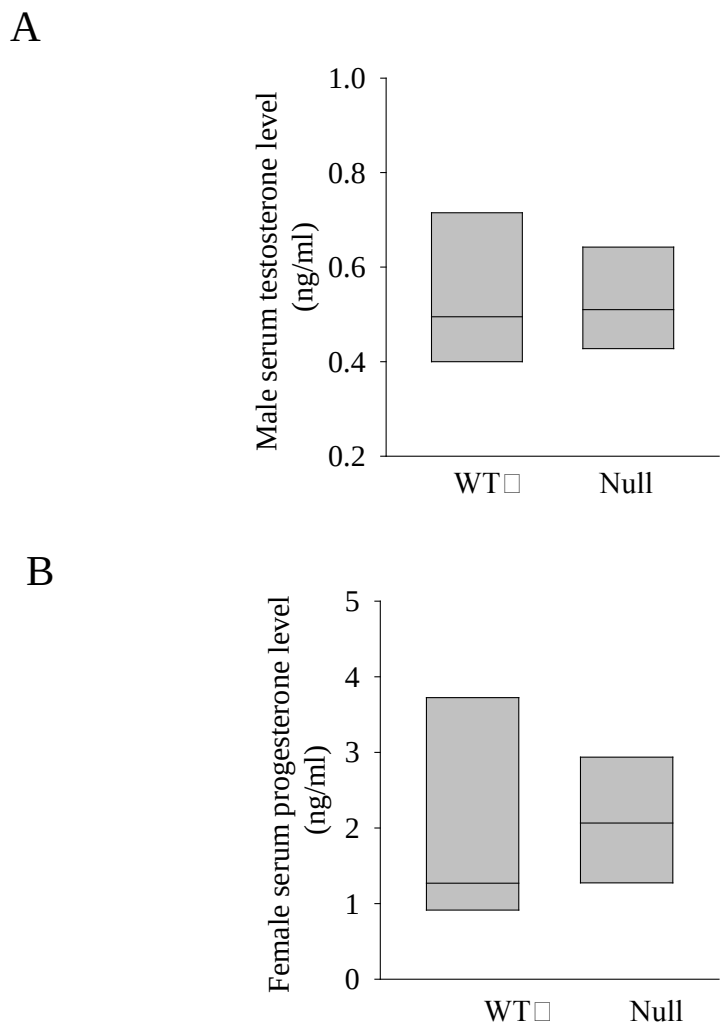

Figure S3. Serum and testosterone and progesterone levels in WT and *Cyp2a5*-null mice. (A). Serum testosterone levels in male mice. (B). Serum progesterone levels in female mice. Testosterone and progesterone levels were determined for 2-month-old male and female mice (n=8), respectively. The values shown are the medians, together with the 25% (lower bar) and 75% (upper bar) percentile marks. No significant difference was found, for testosterone or progesterone levels, between WT and *Cyp2a5*-null groups (Mann-Whitney Rank Sum Test).